Materials Characterization and Device Performance Survey of InAlN/GaN HEMT Layers from Commercial Sources

M. Trejo, G. H. Jessen, A. Crespo, J.K. Gillespie, D. Langley, D. Denninghoff, and G. D. Via
Sensors Directorate, Air Force Research Laboratory
Wright-Patterson Air Force Base, OH 45433

J. Carlin, D. Tomich, J. Grant, and H. Smith
Materials Directorate, Air Force Research Laboratory
Wright-Patterson Air Force Base, OH 45433

Keywords: HEMT, InAlN, wide bandgap, Ka-band

ABSTRACT

In this work, we compare the most recent efforts to develop device-quality InAlN/GaN HEMT structures from three commercial sources. These structures were grown by MOCVD on SiC substrates and all had the same nominal thickness and mole fraction. Device data from two- and four-finger HEMTs will be presented for each material source. We will show the trends observed in the dc, small-signal, and load-pull data as a function of the material stoichiometry, and an estimate of the barrier layer bandgap

INTRODUCTION

There is a need to increase the frequency of wide bandgap devices for millimeter wave power applications. Currently, AlGaN/GaN device layers are grown on SiC substrates for high power devices [1-3]. This device technology relies on spontaneous charge accumulation as well as the lattice mismatch of AlGaN to GaN for piezoelectric charge accumulation [4]. Although AlGaN/GaN HEMTs have demonstrated great potential, limitations of AlGaN barriers still exist. In order to achieve desired current levels, the barrier thickness of AlGaN/GaN devices commonly exceeds 160 Å causing undesirable short-channel effects or the need for a gate recess etch [5]. Additionally, lattice-mismatch-induced strain on the barrier–buffer interface potentially poses limitations on device performance, repeatability, and reliability. The development of an InAlN barrier layer offers a solution to the strain and barrier thickness problem. The advantages of InAlN/GaN HEMTs are still being explored. However, the devices appear especially promising for the realization of high-power electronic devices operating at frequencies greater than Ka-band.

The goal of this work is to assess the current state of InAlN material available from some commercial sources. Preliminary results indicate a wide range of unintentional Ga incorporation into the InAlN barrier from near impurity levels to gross contaminant. An effort was made by the commercial sources to decrease Ga growth on their samples while increasing the In and Al concentration, all while maintaining an unstrained interface. Although the samples provided are quaternary in composition, this study tracks the progress of the device performance as material growth efforts aim towards becoming a ternary HEMT device.

EXPERIMENT

InAlN/GaN HEMT devices fabricated on SiC substrates with similar gate lengths of 150nm ±25nm were investigated. In order to compare similar device structures, InAlN barrier thicknesses ranging from 110-140Å were used (Table I). The material was grown by MOCVD on 6H-SiC substrates.

Prior to device fabrication, in-house and contracted XPS, SIMS, and RBS material composition measurements were performed on test wafers from similar InAlN growth runs. The measured material compositions obtained provided a basis of comparison for this experiment (Table I).

The wafers were processed by contact lithography using a standard high performance device mask. The process included mesa isolation, ohmic contact formation, metal contact deposition, e-beam lithography for T-gates, Si_3N_4 passivation deposition and etch, and post and bridge metal deposition for 4-finger devices. Mesa isolation was achieved using a standard BCl_3 recipe in a PlasmaTherm 770 ICP system. A standard Ti/Al/Ni/Au stack alloyed at 850 °C for 30 sec was used for the ohmic contact formation on all wafers. Si_3N_4 was deposited using a PlasmaTherm 790 PECVD process and was etched using the PlasmaTherm 790 RIE. The identical standard Ni/Au metal stack was used for all of the gates.

MEASUREMENTS AND DISCUSSION

Full wafer measurements were taken at all steps of the process. Each wafer contained between 64-144 sites. Sheet resistance (R_{sh}) and ohmic contact resistance (R_c)

TLM measurements were made using an automated Keithley 450 parameter analyzer. After gate metal deposition, the two-finger devices were measured using an automated test setup consisting of an HP8510 and HP4142 network and parameter analyzers with a Cascade Microtek 12K prober. After passivation, R_{sh} and R_c TLM measurements were repeated on the devices and the PCM structures. After final front side processing, large area devices were probed with the Maury Microwave load pull system.

Full wafer testing of small-signal and dc data were obtained from all the samples (Table I). The two-finger devices were tested from 1–26GHz at 0–10V V_{ds} from 1V to below threshold. Breakdown voltage was tested at 1 mA/mm with a maximum measurable V_{BK} of 50V.

Device performance for f_T and f_{max} was in the range of 35 – 60 GHz and 45 – 84 GHz respectively. The highest I_{DSS} (V_{GS} = 0 V) value observed was 1287.59 mA/mm, and the highest I_{max} (V_{GS} = +1 V) value observed was 1469.39 mA/mm. There was no specific trend correlating frequency or current to the InAlN barrier thickness or material composition.

The total estimated bandgap was derived from the In, Al, and Ga material contribution percentages obtained from the XPS, SIMS, and RBS measurements. Device performance as a function of bandgap and mole fraction provided observable trends. The most noticeable trend was an increase in $|V_{TH}|$ as E_g increased (Fig. 1a). Since the Al contribution ranged between 58%-86% (Table I), it is the major contributor to the total bandgap. As a result, $|V_{TH}|$ increases as a function of Al concentration (Fig. 1b). As the commercial sources attempted to eliminate the Ga incorporation into their samples, they also sought to increase the In and Al concentrations. The results of this attempt are noticeable in Fig. 1c which indicates higher $|V_{TH}|$ and R_c as the Ga content decreases. Source B, which provided samples with less Ga incorporation and greater In and Al concentration demonstrated higher $|V_{TH}|$ with a maximum $|V_{TH}|$ of 6.67V with 9% In and 86 % Al An interesting observation is the increase in R_c as a function of higher In concentration (Fig. 1d). However, the samples with the highest In concentration also had the highest Al concentration. Source B had the highest average R_c of 4.94Ω-mm indicating that the larger bandgap of the barrier layer does indeed affect the contact resistance. Source A samples had transconductance in the range of 362 mS/mm-483 mS/mm while g_m values for samples from sources B and C did not exceed 300mS/mm. Based on the observed data from the three sources, there was no clear correlation between R_{sh} and the stoichiometry of the material in any of the samples.

Load pull measurements were taken at Ka-band with V_{ds}=20V and at a 25% I_{dss} operating point. Maximum power, efficiency, and gain data was obtained from 4-finger HEMT devices with L_g = 150nm and W_g = 85µm (Table I). Load pull data optimized for maximum power from all three sources indicates a maximum power output range between 0.99 W/mm and 4.28 W/mm at 35GHz. In addition, PAE and G_t were in the range of 13.1% – 26.6% and 5.56dB – 9.26dB respectively. The power measurements indicate that there is no apparent dependency on material composition but may have a relationship to material growth conditions and material defects.

CONCLUSION

We reported on the differences observed between the device performance and material characterization for structures processed on commercially obtained InAlN/GaN epitaxial material. The preliminary data demonstrates that expected benefits of InAlN are not observed in greater I_{DSS} and I_{max} mostly due to lower than expected mobility. Furthermore, we find that stoichiometry of the material is not a primary limitation. Instead, unknown material defects and interface quality do present a greater limitation to device performance. To gain a better understanding of the current state of InAlN material technology, further material development is needed as well as an ohmic metal optimization study for wider bandgap InAlN layers to be able to demonstrate improvements in device performance.

ACKNOWLEDGEMENTS

Authors would like to acknowledge Paul Cassity and Joe Breedlove for their etching and metal deposition services.

REFERENCES

[1] T. Palacios, A. Chakraborty, S. Rajan, C. Poblenz, S.Keller, S. P. DenBaars, J. S. Speck, and U. K. Mishra, "High-power AlGaN/GaN HEMTs for Ka-band applications," *IEEE Electron Device Letters*, vol. 26, no. 11, pp. 781-783, Nov. 2005.

[2] Y.-F Wu, A. Saxler, M. Moore, R. P. Smith, S. Sheppard, P. M. Chavarkar, T. Wisleder, U. K. Mishra, and P. Parikh, "30-W/mm GaN HEMTs by field plate optimization," *IEEE Electron Device Letters*, vol. 25, no. 3, pp. 117-119, Mar. 2004.

[3] M. Higashiwaki, T. Mimura, and T. Matsui, "High-Performance Short-Gate InAlN/GaN Heterostructure Field-Effect Transistors," *Japanese Journal of Applied Physics*, vol. 45, no. 32, pp. L843-L845, 2006.

[4] J. Kuzmik "Power Electronics on InAlN/(In)GaN:Prospect for a Record Performance" *IEEE Electron Device Letters*, vol. 22, no. 11, pp. 510-512, Nov. 2001.

[5] G. Jessen, R. Fitch, J. Gillespie, G.D. Via, A. Crespo, D. Langley, D.J. Denninghoff, M. Trejo, and E.R. Heller, " Short-Channel Effect Limitations in High-Frequency Operation of AlGaN/GaN HEMTs for T-Gate Devices," IEEE Transactions on Electronic Devices, vol. 54, no. 10, pp. 2589-2597, 2007.

ACRONYMS

HEMT: High Electron Mobility Transistor
XPS: X-Ray Photoelectron Spectroscopy
SIMS: Secondary Ion Mass
RBS: Rutherford Backscatter
PECVD: Plasma Enhanced Chemical Vapor Deposition
MOCVD: Metal Organic Chemical Vapor Deposition
RIE: Reactive Ion Etch
ICP: Induced Coupled Plasma

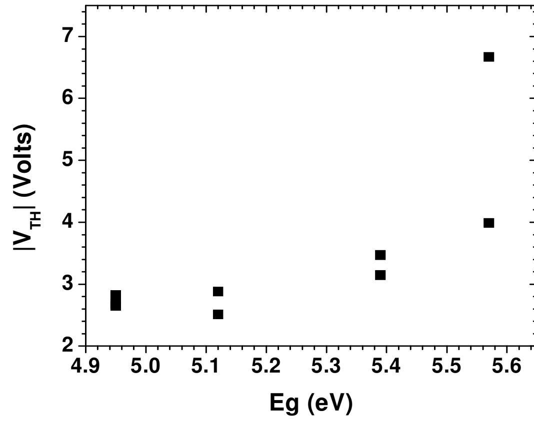

(a)

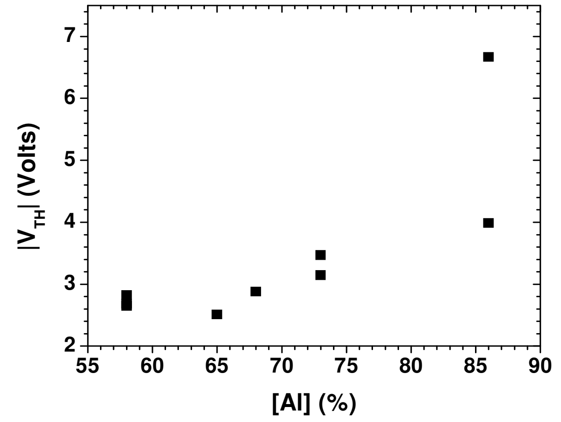

(b)

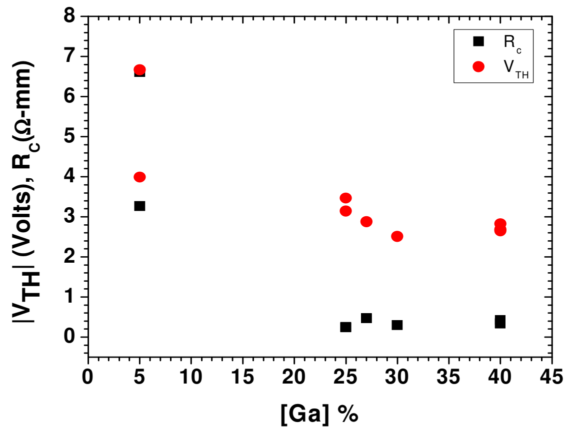

(c)

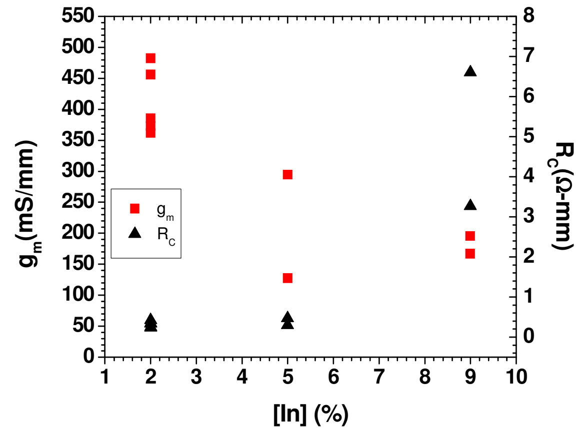

(d)

Fig. 1. Observable trends in the data analysis with respect to average bandgap (E_g) and material composition percentages. (a) increasing V_t as a function of E_g (b) increasing V_t as Al % increases (c) decreasing V_t and R_c as Ga% increases (d) decreasing g_m and increasing R_c as In % increases

TABLE I
AVERAGE FULL-WAFER DC AND SMALL SIGNAL DATA AND MAXIMUM POWER MEASUREMENTS FOR InAlN/GaN HEMTs PROCESSED ON SAMPLES WITH VARIED InAlN BARRIER LAYERS FROM THREE COMMERCIAL SOURCES

Source	**A**					**B**		**C**	
Sample ID	**1**	**2**	**3**	**4**	**5**	**6**	**7**	**8**	**9**
L_g (nm)	150	150	150	125	125	150	150	125	125
T_{bar} (Å)	110	125	134	116	120	120	140	120	120
In %	2	2	2	2	2	9	9	5	5
Al %	58	58	58	73	73	86	86	68	68
Ga %	40	40	40	25	25	5	5	27	27
Average DC and Small Signal Data									
R_c (Ω-mm)	0.43	0.334	0.345	0.256	0.238	3.27	6.61	0.47	0.298
R_{sh} (Ω/sq)	317.0	307.1	346.7	232.9	229.6	649.3	284.1	399.0	338.4
$\lvert I_{gl} \rvert$ (mA)	0.2348	0.0434	0.0019	0.0049	0.0803	0.9232	0.0571	0.0229	0.015
f_T (GHz)	46.38	49.49	50.23	53.58	60.07	47.669	49.98	35.34	49.41
f_{max} (GHz)	47.87	74.23	73.39	80.27	80.65	75.07	83.71	52.62	45.3
g_m (mS/mm)	372.89	361.88	385.55	456.18	482.6	167.11	195.5	127.49	294.55
$\lvert V_t \rvert$ (V)	2.683	2.823	2.65	3.145	3.467	6.668	3.989	2.879	2.51
I_{max} (mA/mm)	1091.78	1093.87	1093.46	1395.19	1469.39	1117.37	824.11	339.64	679.92
V_{bk} (V)	4.87	24.69	24.88	11.38	21.39	8.898	5.122	0.957	9.954
I_{dss} (mA/mm)	896.75	914.96	893.8	1191.63	1287.59	1029.46	736.51	282.38	559.35
h21	64.76	47.21	48.21	52.14	59.18	40.99	43.13	32.39	60.4
E_g (eV)	4.95	4.95	4.95	5.39	5.39	5.57	5.57	5.12	5.12
Maximum Power Data									
PAE (%)	26.6	13.8	17.5	14.6	20.4	13.1	20.6	N/A	20.9
P_{out} (W/mm)	2.3	3.28	0.99	3.37	4.28	1.75	3.63	N/A	1.68
G_t (dB)	9.11	6.13	5.82	7.68	9.26	5.56	7.05	N/A	7.54